Journal of *Marine Science and Engineering*

MDPI

Article

Simplified Target Strength Analysis Procedure of an Underwater Vehicle Considering Target Strength Absorbing Materials

Jangwoo Kim [1,†], Jaeman Kim [2,†], Joo-Yeob Lee [3], Dae-Seung Cho [1,3], Sung-Ju Park [4,5], Kyungjun Song [2,*], Yun-ho Shin [1,3,5,*] and Kookhyun Kim [5,6,*]

1 Department of Naval Architecture and Ocean Engineering, Pusan National University, Busan 46241, Republic of Korea; koyaddr@pusan.ac.kr (J.K.); daecho@pusan.ac.kr (D.-S.C.)
2 School of Mechanical Engineering, Pusan National University, Busan 46241, Republic of Korea; jaeman101@pusan.ac.kr
3 Global Core Research Center for Ships and Offshore Plants (GCRC-SOP), Pusan National University, Busan 46241, Republic of Korea; hermedo@pusan.ac.kr
4 School of Electrical & Control Engineering, Tongmyong University, Busan 48520, Republic of Korea; parksj0314@tu.ac.kr
5 Open Grid Laboratory, Busan 48520, Republic of Korea
6 Advanced Defense Engineering Course, Graduate School of Changwon National University, Changwon 51140, Republic of Korea
* Correspondence: song3396@pusan.ac.kr (K.S.); shinyh77@pusan.ac.kr (Y.-h.S.); kimk@changwon.ac.kr (K.K.); Tel.: +82-51-510-2986 (K.S.); +82-51-510-2441 (Y.-h.S.); +82-51-629-1658 (K.K.)
† These authors contributed equally to this work as the first author.

Abstract: Target strength (TS) is an important design factor for improving the survivability of an underwater vehicle, and various efforts are ongoing to enhance it. Among the design techniques to improve TS, absorbing materials attached to the surface of an underwater vehicle can play a key role by reducing the reflected and scattered acoustic waves. In this study, the acoustic performance of target strength absorbing materials (TSAMs) is first analyzed, and then the simplified procedure of TS analysis considering TSAMs is suggested. The 4-microphone method and transfer matrix method evaluating equivalent material properties of TSAMs are derived, and their effectiveness is cross-validated through a series of analyses for a multi-layer acoustic absorbing structure. From the observed results, it is concluded that the transfer matrix method is more suitable for practical TS analysis than the 4-microphone method because of the relatively low calculation and time costs required for the acoustic performance evaluations of TSAMs. In addition, a simplified TS analysis procedure considering the echo reduction (ER) and transmission loss (TL) is proposed based on the combining method of physical optics and geometric optics (PO/GO combined method) and equivalent material properties. Using the suggested procedure, a series of TS analyses are performed using the Benchmark Target Strength Simulation (BeTSSi) to validate its applicability and effectiveness.

Keywords: underwater vehicle; target strength (TS); target strength absorbing material (TSAM); echo reduction (ER); transmission loss (TL)

check for updates

Academic Editors: Giulia Palomba and Pasqualino Corigliano

Received: 30 November 2024
Revised: 23 December 2024
Accepted: 24 December 2024
Published: 1 January 2025

Citation: Kim, J.; Kim, J.; Lee, J.-Y.; Cho, D.-S.; Park, S.-J.; Song, K.; Shin, Y.-h.; Kim, K. Simplified Target Strength Analysis Procedure of an Underwater Vehicle Considering Target Strength Absorbing Materials. *J. Mar. Sci. Eng.* **2025**, *13*, 62. https://doi.org/10.3390/jmse13010062

Copyright: © 2025 by the authors. Licensee MDPI, Basel, Switzerland. This article is an open access article distributed under the terms and conditions of the Creative Commons Attribution (CC BY) license (https://creativecommons.org/licenses/by/4.0/).

1. Introduction

The survivability of underwater platforms such as submarines is heavily dependent on stealth techniques that make it difficult for the enemy to detect and track them. Target strength (TS) is one of the key indicators for assessing low detectability, that is, susceptibility, and extensive research has been accomplished during the design phase to reduce it [1,2]. Among them, target strength absorbing materials (TSAMs) are attached to the surface of

the underwater vehicle to increase its survivability. TSAMs are designed to absorb an acoustic wave from active sound navigation and ranging (SONAR) and reduce the reflected wave. Underwater acoustic absorbing material have evolved from Alberich coatings [3–5], which are pores embedded in viscoelastic materials represented by rubber, to multi-layer structure [6] that can operate in different frequency bands, and now there is a lot of research on acoustic meta-absorbers using meta-structures [7–10] or meta-materials [11,12] that exhibit effective acoustic performance in low frequencies or broadbands. Therefore, to conduct a TS analysis closer to reality, it is important to consider the acoustic performance of TSAMs when analyzing the TS of an underwater vehicle.

Because the types of underwater acoustic absorbing material are diverse and they are still being developed, various methods to analyze the acoustic performance have been developed. Typical methods are using acoustic tank [13] and waveguide [14,15], and in the case of waveguide, the 2- or 4-microphone method [16,17] and transfer matrix method [18–20] are mainly used. These methods for acoustic performance analysis are used not only to analyze the acoustic performance of acoustic absorbing material, but also to calculate the factors for analyzing TS of ships or equipment.

Regarding the TS analysis method, an analytical solution of TS for simple geometries such as flat plates, cylinders, and spheres is well known and easily approached [21]. Numerical methods for TS analysis include a low-frequency analysis method such as the boundary element method (BEM) [22], and a finite element method (FEM) [23], as well as a high-frequency analysis method like physical optics (PO) [24–26], geometric optics (GO) [27] or physical theory of diffraction (PTD) [28]. Low-frequency analysis methods can provide highly accurate solutions for arbitrary geometries, but the computational burden and errors increase with the size of the target. Therefore, high-frequency methods are mainly applied for the TS analysis of large and complex underwater targets [29]. Most of the studies have analyzed the TS of underwater vehicles by assuming the target as a perfect reflector. In addition, while many studies have evaluated the performance of TSAM itself, the study by Kwon et al. [30] used the finite element method (FEM) to analyze the acoustic reflection and transmission coefficients of Alberich anechoic coatings, a type of TSAM, applied to underwater vehicles. This study considered the reflection coefficients utilizing the acoustic impedance of the analyzed coatings during TS analysis, but energy losses were neglected when acoustic waves were transmitted through the outer structure of the vehicle into its inner structures. In summary, while studies on specific TS analysis methodologies have been accomplished, as described above, studies establishing overall TS analysis procedures, including TSAM, have been relatively rare.

In this study, a simplified TS analysis procedure considering echo reduction (ER) and transmission loss (TL) is proposed based on the combined methods of physical optics and geometric optics (PO/GO combined method), as well as equivalent material properties. The 4-microphone method and transfer matrix method evaluating equivalent material properties of TSAMs are derived, and their effectiveness is cross-validated through a series of analyses for a multi-layer acoustic absorbing structure. Then, a series of numerical analyses of TS based on the PO/GO combined method of the standard model, Benchmark Target Strength Simulation (BeTSSi), which is used in the TS analysis of underwater vehicles, are performed using the proposed procedure to show its effectiveness.

The methods for calculating acoustic performance of TSAMs for TS analysis are first dealt with in Section 2 and then the simplified analysis procedure considering TSAMs is suggested in Section 3. The acoustic performance of TSAMs using the methods in Section 2 is cross-validated through a series of analyses for a multi-layer acoustic absorbing structure in Section 4, and the numerical analyses of TS based on the PO/GO combined method of

the BeTSSi model are described to show the effectiveness of the suggested procedure in Section 5.

2. Methodology of Calculating Acoustic Performance of Target Strength Absorbing Material for Target Strength Analysis

2.1. ER and TL Calculation by 4-Microphone Method

The 4-microphone method is a method for measuring the acoustic performance of acoustic absorbing material located inside a waveguide with a constant cross-sectional area and cross-sectional geometry using four acoustic microphones. Figure 1 shows a schematic diagram of a waveguide with the 4-microphone method.

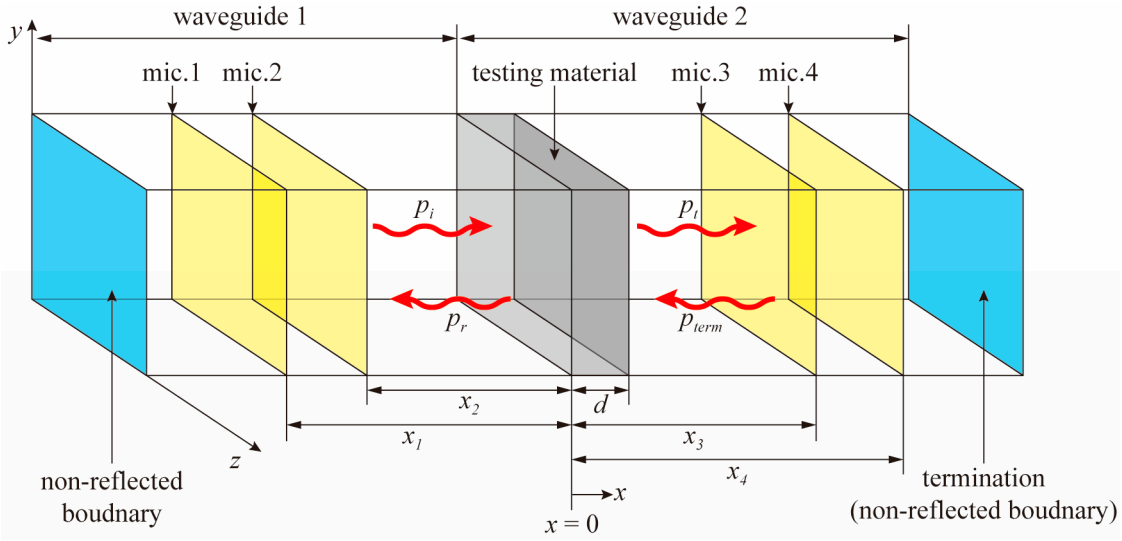


Figure 1. Schematic diagram of the waveguide with the 4-microphone method.

A plane wave propagating in a waveguide is divided into an incident wave (p_i), a reflected wave in waveguide 1 (p_r), a transmitted wave (p_t), and a reflected wave in waveguide 2 (p_{term}) due to reflection and transmission at the testing material and the termination of the waveguide. The p_i, p_r, p_t and p_{term} are measured by acoustic microphones attached to the waveguide. It is assumed that the acoustic wave propagating in the waveguide has the form of a harmonic function; the acoustic pressure measured by the n-th microphone is expressed as:

$$p(x,\omega) = P_n e^{j\omega t} = \left(Ae^{-jkx} + Be^{jkx}\right)e^{j\omega t} \tag{1}$$

where P_n is the amplitude of the acoustic pressure measured at the n-th microphone, $e^{j\omega t}$ is the phase in time and $e^{\pm jkx}$ is the phase in space where k is wavenumber and ω is angular frequency. A and B are the amplitudes of the acoustic pressure. The acoustic pressure measured by each microphone is expressed as follows:

$$P_1 e^{j\omega t} = P_i e^{j(-kx_1+\omega t)} + P_r e^{j(kx_1+\omega t)}, \tag{2}$$

$$P_2 e^{j\omega t} = P_i e^{j(-kx_2+\omega t)} + P_r e^{j(kx_2+\omega t)}, \tag{3}$$

$$P_3 e^{j\omega t} = P_t e^{j(-kx_3+\omega t)} + P_{term} e^{j(kx_3+\omega t)}, \tag{4}$$

$$P_4 e^{j\omega t} = P_t e^{j(-kx_4+\omega t)} + P_{term} e^{j(kx_4+\omega t)} \tag{5}$$

Therefore, P_i, P_r, P_t, and P_{term}, are expressed as follows:

$$P_i = j\frac{P_1 e^{jkx_2} - P_2 e^{jkx_1}}{2\sin k(x_1 - x_2)}, \tag{6}$$

$$P_r = j\frac{P_2 e^{-jkx_1} - P_1 e^{-jkx_2}}{2\sin k(x_1 - x_2)}, \tag{7}$$

$$P_t = j\frac{P_3 e^{jkx_4} - P_4 e^{jkx_3}}{2\sin k(x_3 - x_4)}, \tag{8}$$

$$P_{term} = j\frac{P_4 e^{-jkx_3} - P_3 e^{-jkx_4}}{2\sin k(x_3 - x_4)} \tag{9}$$

As described in Equations (6)–(9), the amplitudes and the phases of the acoustic pressure measured by the microphones can be used to represent the acoustic wave propagating in the waveguide. Because the termination of the waveguide is a non-reflected boundary, as shown in Figure 1, then $P_{term} = 0$. Reflection coefficient and transmission coefficient are represented as $R = \frac{P_r}{P_i}$ and $T = \frac{P_t}{P_i}$, respectively. The ER and TL are expressed as follows:

$$ER = 10\log_{10}\left|\frac{1}{r}\right|, \tag{10}$$

$$TL = 10\log_{10}\left|\frac{1}{\tau}\right|, \tag{11}$$

where $r = |R|^2$ is power reflection coefficient and $\tau = |T|^2$ is power transmission coefficient.

2.2. ER and TL Calculation by Transfer Matrix Method

Acoustic absorbing materials with multi-layer structures or complex geometries are difficult to analyze using theoretical approaches. For ease of analysis, acoustic absorbing materials can be expressed in terms of equivalent properties that show the same acoustic performance. This method is called transfer matrix method, which is applicable when the thickness of the acoustic absorbing material is relatively small compared to the wavelength scale.

As shown in Figure 2, p_i and p_r propagate in medium 1, and p_t propagates in medium 2. Due to the different acoustic wave propagations in each medium, acoustic pressure P and particle velocity u at interfaces at $x = 0$ and $x = d$ are different. A relationship between the acoustic pressure and particle velocity at each interface is given by the transfer matrix as follows:

$$\begin{bmatrix} P \\ u \end{bmatrix}_{x=0} = \begin{bmatrix} T_{11} & T_{12} \\ T_{21} & T_{22} \end{bmatrix} \begin{bmatrix} P \\ u \end{bmatrix}_{x=d} = [T] \begin{bmatrix} P \\ u \end{bmatrix}_{x=d} \tag{12}$$

where $\begin{bmatrix} P \\ u \end{bmatrix}_{x=0}$ and $\begin{bmatrix} P \\ u \end{bmatrix}_{x=d}$ are the acoustic pressure and particle velocity at $x = 0$ and $x = d$, respectively, and $[T]$ is the transfer matrix of the acoustic absorbing material. As shown in Figure 2, p_a is forward wave and p_b is backward wave in the acoustic absorbing material. The acoustic pressure and particle velocity at each interface are expressed as follows:

$$P_{x=0} = P_a + P_b \tag{13}$$

$$u_{x=0} = \frac{1}{\rho c}(P_a - P_b) \tag{14}$$

$$P_{x=d} = P_a e^{-jkd} + P_b e^{jkd} \tag{15}$$

$$u_{x=d} = \frac{1}{\rho c}\left(P_a e^{-jkd} - P_b e^{jkd}\right) \tag{16}$$

where ρ is density and c is wave speed of acoustic absorbing material. Therefore, the transfer matrix between each interface is expressed as:

$$\begin{bmatrix} P \\ u \end{bmatrix}_{x=0} = \begin{bmatrix} \cos kd & jZ\sin kd \\ j\frac{1}{Z}\sin kd & \cos kd \end{bmatrix} \begin{bmatrix} P \\ u \end{bmatrix}_{x=d} \tag{17}$$

where $Z = \rho c$ is acoustic impedance of acoustic absorbing material.

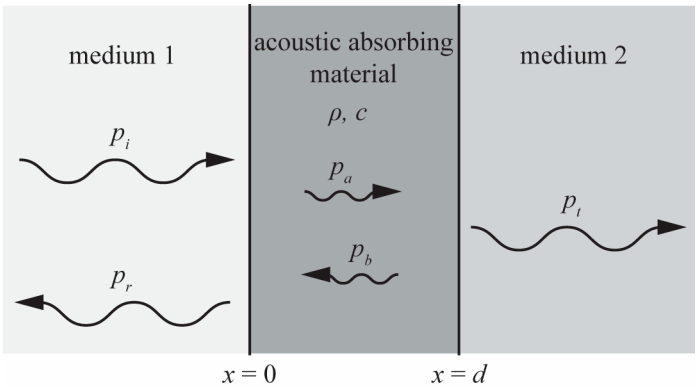


Figure 2. Wave propagation in the external media and inside the acoustic absorbing material.

Transfer matrix $[T]$ for a single layer reflects the coating properties (Z, k) and structure (d). In case the acoustic absorbing material is a multi-layer structure with N layers, or it is analyzed in terms of N layers, each layer has a transfer matrix representing the properties of that layer, resulting in a total of N transfer matrices. The transfer matrix for the entire acoustic absorbing material, $[T]_{total}$, is expressed as:

$$[T]_{total} = \prod_{i=1}^{N} [T]_i = \begin{bmatrix} T_{11,total} & T_{12,total} \\ T_{21,total} & T_{22,total} \end{bmatrix} \tag{18}$$

The elements of the transfer matrix for the entire acoustic absorbing material also have the form of the transfer matrix elements given in Equation (17), so that the equivalent impedance Z_{eq} and equivalent wavenumber k_{eq} are expressed as:

$$Z_{eq} = \sqrt{T_{12,total}/T_{21,total}} \tag{19}$$

$$k_{eq} = \frac{1}{d}\arcsin\sqrt{-T_{12,total}\ T_{21,total}} \tag{20}$$

Using the equivalent properties derived from the transfer matrix method, an acoustic absorbing material composed of layers with different densities, wave speeds and thicknesses shown in Figure 3a can be converted into a single layer acoustic absorbing material with the equivalent impedance and wavenumber as shown in Figure 3b. Reflection coefficient and transmission coefficient in Figure 3b are expressed as follows:

$$R = \frac{\left(1 - \frac{Z_1}{Z_3}\right)\cos k_{eq}d + j\left(\frac{Z_{eq}}{Z_3} - \frac{Z_1}{Z_{eq}}\right)\sin k_{eq}d}{\left(1 + \frac{Z_1}{Z_3}\right)\cos k_{eq}d + j\left(\frac{Z_{eq}}{Z_3} + \frac{Z_1}{Z_{eq}}\right)\sin k_{eq}d} \tag{21}$$

$$T = \frac{2e^{ik_3 d}}{\left(1 + \frac{Z_1}{Z_3}\right)\cos k_{eq}d + j\left(\frac{Z_{eq}}{Z_3} + \frac{Z_1}{Z_{eq}}\right)\sin k_{eq}d} \tag{22}$$

where Z_1 is the acoustic impedance of medium 1 and Z_3 is the acoustic impedance of medium 3. If $Z_1 = Z_3$, R and T are simplified as follows:

$$R = \frac{j\left(\frac{Z_{eq}}{Z_1} - \frac{Z_1}{Z_{eq}}\right)\sin k_{eq}d}{2\cos k_{eq}d + j\left(\frac{Z_{eq}}{Z_1} + \frac{Z_1}{Z_{eq}}\right)\sin k_{eq}d} \tag{23}$$

$$T = \frac{2e^{ik_3 d}}{2\cos k_{eq}d + j\left(\frac{Z_{eq}}{Z_1} + \frac{Z_1}{Z_{eq}}\right)\sin k_{eq}d} \tag{24}$$

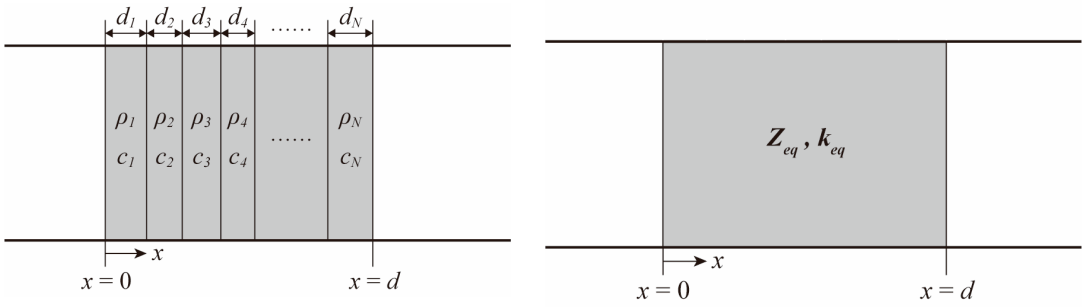


Figure 3. Acoustic absorbing material of (**a**) multi-layer structure, (**b**) single layer with equivalent properties.

3. Suggestion of a Simplified TS Analysis Procedure

3.1. Overview of Target Strength Analysis Theory

In this study, the PO/GO combined method [29], which has been effectively and frequently used for TS analysis, was adopted to propose the simplified analysis procedure of an underwater vehicle considering the TSAMs. In this section, the frequency-domain-based physical optics theory used in this method is explained. The theory is derived from the Kirchhoff–Helmholtz integral equation by applying the Kirchhoff approximation theory.

The pressure at the arbitrary location scattered from the target in the frequency domain is derived from the Kirchhoff–Helmholtz integral equation, which is described in Equation (25), assuming that the acoustic wave is incident toward the center of the target in the form of a plane wave, as shown in Figure 4.

$$P_s\left(\vec{r},\omega\right) = \int_S \left[G\left(\vec{r},\vec{r}'\right)\frac{\partial P\left(\vec{r}'\right)}{\partial n} - P(\vec{r}')\frac{\partial G\left(\vec{r},\vec{r}'\right)}{\partial n}\right] dS \tag{25}$$

where $P_s\left(\vec{r},\omega\right)$ denotes the pressure response scattered from the target at an arbitrary receiver position, $\vec{r}$, in the frequency, domain and $P\left(\vec{r}'\right)$ is the pressure response induced by the incidence and scattering at an arbitrary position vector $\vec{r}'$ on the target surface. In addition, $G\left(\vec{r},\vec{r}'\right)$ and $\frac{\partial G\left(\vec{r},\vec{r}'\right)}{\partial n}$ mean the Green function and its partial derivative with respect to the normal direction of the target surface, respectively, and they can be approximated, as described in Equations (26) and (27), under the assumption of the far-field condition, $r \to \infty$.

$$G\left(\vec{r},\vec{r}'\right) = \frac{e^{-j\vec{k}_s\cdot(\vec{r}-\vec{r}')}}{4\pi\left|\vec{r}-\vec{r}'\right|} \approx \frac{e^{-jkr}}{4\pi r}e^{j\vec{k}_s\cdot\vec{r}'} \tag{26}$$

$$\frac{\partial}{\partial n}G\left(\vec{r},\vec{r}'\right) = -\left(jk+\frac{1}{r}\right)\cos\phi_s G\left(\vec{r},\vec{r}'\right) \approx -jk\cos\phi_s G\left(\vec{r},\vec{r}'\right) \tag{27}$$

where r is the distance between the origin of the coordinate system and the receiver, $\left|\vec{r}'\right|$, k_s is the magnitude of wave number, $\left|\vec{k}_s\right|$, and ϕ_s is the angle between unit normal vector $\hat{n}$ to the target plane and the scattering direction vector, $\vec{r} - \vec{r}'$.

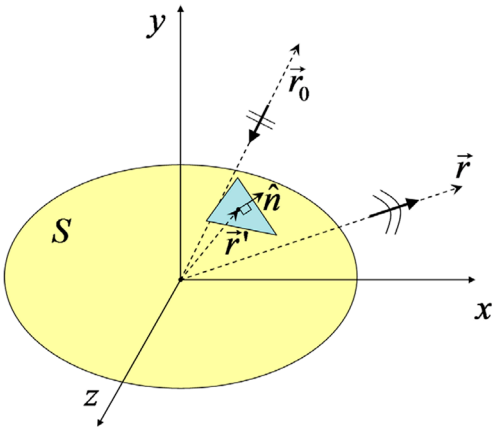


Figure 4. Acoustic waves incident and scattered on a target surface and coordinate system.

The pressure $P\left(\vec{r}'\right)$ is expressed as the summation of the incident and scattered pressure at an arbitrary location on the target plane and $P_i\left(\vec{r}'\right)$ and $P_s\left(\vec{r}'\right)$ are from the Kirchhoff approximation theory and their partial derivatives, and themselves are approximated under the assumption of the plane wave, i.e., far-field conditions, as below:

$$P\left(\vec{r}'\right) = P_i\left(\vec{r}'\right) + P_s\left(\vec{r}'\right) \tag{28}$$

$$P_i\left(\vec{r}'\right) = P_0\left(\vec{r}_0,\omega\right)e^{j\vec{k}_i\cdot\vec{r}'} \tag{29}$$

$$\frac{\partial}{\partial n}P_i\left(\vec{r}'\right) \approx -jk\cos\phi_i P_i\left(\vec{r}'\right) \approx -jk\cos\phi_i P_0\left(\vec{r}',\omega\right)e^{j\vec{k}_i\cdot\vec{r}'} \tag{30}$$

$$P_s\left(\vec{r}'\right) = \Gamma P_i\left(\vec{r}\right) = \Gamma P_0\left(\vec{r}_0,\omega\right)e^{j\vec{k}_i\cdot\vec{r}'} \tag{31}$$

$$\frac{\partial}{\partial n}P_s\left(\vec{r}'\right) \approx -\Gamma\frac{\partial}{\partial n}P_i\left(\vec{r}'\right) \approx jk\cos\phi_i\Gamma P_0\left(\vec{r}',\omega\right)e^{j\vec{k}_i\cdot\vec{r}'} \tag{32}$$

where $\vec{r}_0$ denotes the position vector of the transmitter and Γ denotes the complex reflection coefficient for the angle ϕ_i between the normal vector $\hat{n}$ of the target surface and the incident direction vector $\vec{r}_0 - \vec{r}'$.

Addressing the finite-element-based approach for the target in Figure 5 and assuming the source and receiver as the same positions along the z-axis, Equation (25) can be described as below under the conditions of Equation (33):

$$\phi_i = \phi_s = \phi,\ \vec{k}_i = -\vec{k}_s,\ \vec{k}_s\cdot\left(\vec{r} - \vec{r}'\right) = r - z',\ \vec{r}_0 = \vec{r} \tag{33}$$

$$P_s\left(\vec{r},\omega\right) = -\frac{jk}{2\pi r}P_0\left(\vec{r},\omega\right)e^{jkr}\sum_{m=1}^{M}\Gamma_m\int_{S_m}e^{2jkz'}\cos\phi_m dS \tag{34}$$

where M denotes the total number of 2D elements comprising the target, and Γ_m and S_m are the complex reflection coefficient and the surface of each element, respectively. ϕ_m

means the angle between the unit normal vector of the m-th triangular element and the incident direction vector $\vec{r} - \vec{r}'$. The analytic solution for the phase integration, including its derivation procedure, is explained in reference [26] in detail.

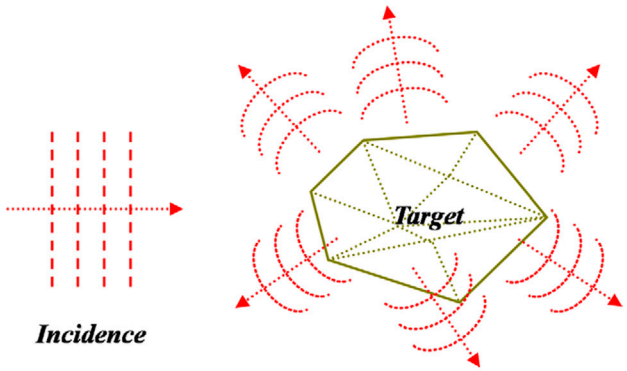


Figure 5. Target divided into a finite number of triangular elements.

Meanwhile, the Kirchhoff approximation theory assumes that only the portions of the target surface directly illuminated by the acoustic energy contribute to the TS, necessitating the application of an appropriate method. Therefore, in this study, the TS analysis applies the PO/GO combined method, including Snell's law, to account for the multiple reflection effects of underwater vehicles. This method applies physical optics to the final reflection surface and geometric optics to the earlier reflection surfaces. In the application of the proposed procedure in Section 5, the TS of the underwater vehicles assumed to be a perfect reflector was analyzed using SYSCOS software, which was developed for complex object scattering analysis based on this method. The detailed description of the proposed simplified TS analysis procedure using this method is provided in Section 3.2.

3.2. Simplified Target Strength Analysis Procedure Considering Target Strength Absorbing Material

In this study, a simplified TS analysis procedure is suggested, which evaluates the TS of underwater vehicles by considering the acoustic performance of TSAMs. The suggested overall TS analysis procedure is illustrated in Figure 6.

The suggested procedure is separated as outer and inner structure analysis of the underwater vehicle to effectively consider the ER and TL. The TS is first analyzed based on the PO/GO combined method described in Section 3.1 for each structure, where the target surface of each structure is assumed to be a perfect reflector. The assumption of a perfect reflector makes it difficult to accurately consider the acoustic properties of the materials that constitute the actual external surface of the underwater vehicle. To address this limitation, the proposed procedure reflects the acoustic properties of the surface materials by calculating ER and TL, as described in Equations (10) and (11), respectively.

For the outer structure, it is necessary to consider the ER of the TSAM that forms the surface, as shown in Figure 7, when acoustic waves are incident on the structure from underwater. Elements that require consideration of sound absorption characteristics are classified and the equivalent material properties of TSAM are applied to elements to which sound absorbing materials are applied. The TS of the outer structure is therefore calculated by considering both the TS derived under the assumption of perfect reflector and the ER of the TSAM.

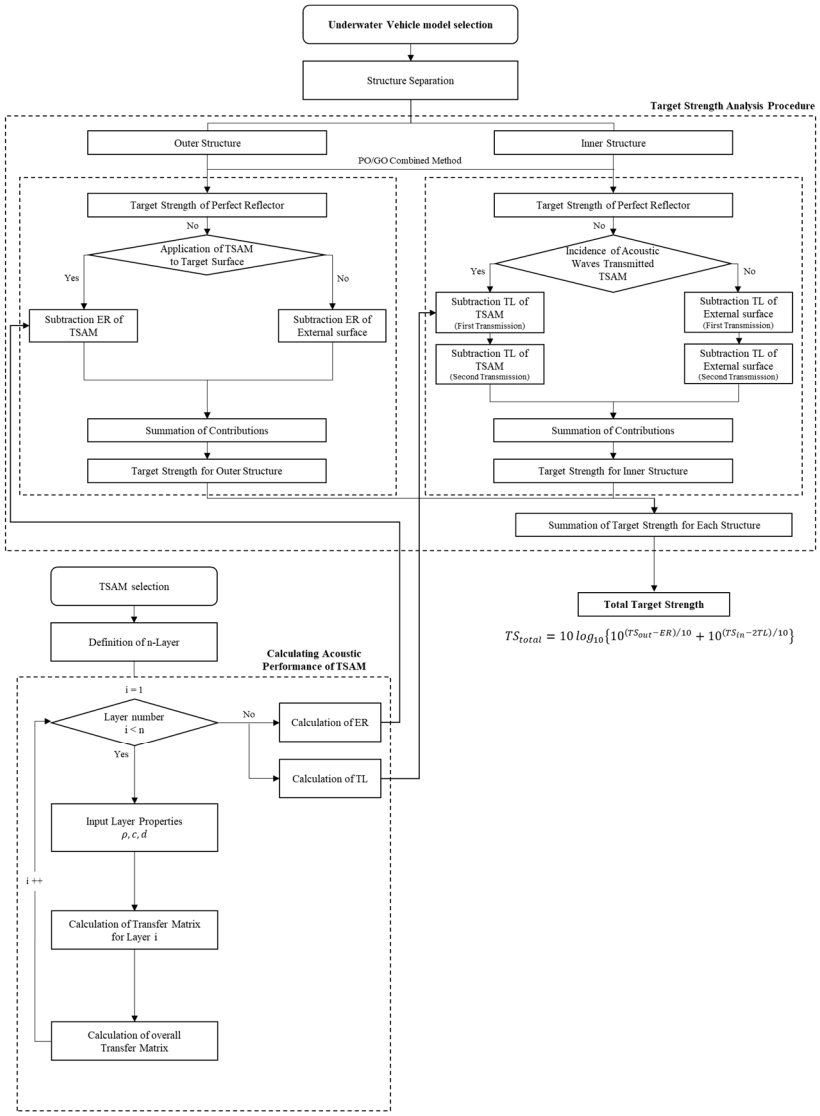


Figure 6. Simplified target strength analysis procedure of an underwater vehicle considering yjr equivalent material property of TSAM.

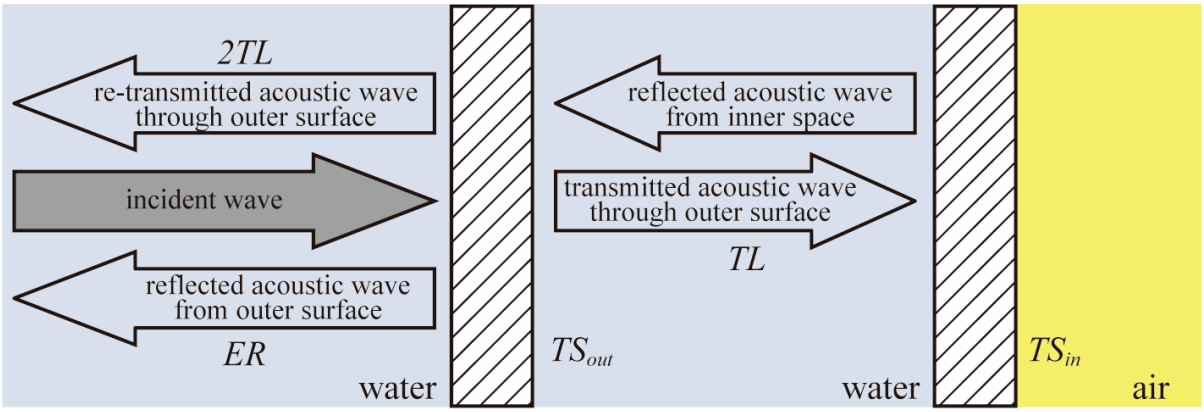


Figure 7. Acoustic waves incident reflected and transmitted into an underwater vehicle and ER and TL.

For the inner structure, acoustic waves are first transmitted through the outer structure and then incident on the inner structure. The waves reflected by the inner structure are then transmitted back through the outer structure before radiating into the underwater,

as shown in Figure 7. This process involves double transmission, leading to the loss of acoustic energy. Therefore, the TS of the inner structure is calculated by considering both the TS derived under the assumption of perfect reflector and two times of transmission loss due to TSAM.

The total TS of the underwater vehicle is calculated by summing the TS of the outer structure, which considers the ER for the selected sections, and the TS of the inner structure, which considers twice the TL for the selected sections. The TSs of the outer and inner structures are summed logarithmically, as described in Equation (35), to consider the actual physical quantities of each structure.

$$TS_{total} = 10\log_{10}\left\{10^{(TS_{out}-ER)/10} + 10^{(TS_{in}-2TL)/10}\right\} \quad (35)$$

where TS_{total} denotes the TS for the entire underwater vehicle, TS_{out} is the TS for the outer structure of the underwater vehicle assuming the target surface is a perfect reflector, TS_{in} is the TS for the inner structure of the underwater vehicle assuming the target surface is a perfect reflector, and ER and TL are the echo reduction and transmission loss, respectively.

4. Cross-Validation of TSAM Performance Analysis Methods

4.1. Analysis Methods, Model, and Conditions

In this study, a 4-microphone method (4MM) and transfer matrix method (TMM) evaluating acoustic performances of TSAMs are cross-validated via a series of numerical analyses for a 10-layer acoustic absorbing material (10LAAM) shown in Figure 8. The properties of each layer of the 10LAAM are set to have a gradually increasing impedance. Details on the properties and thickness of each layer are represented in Table 1.

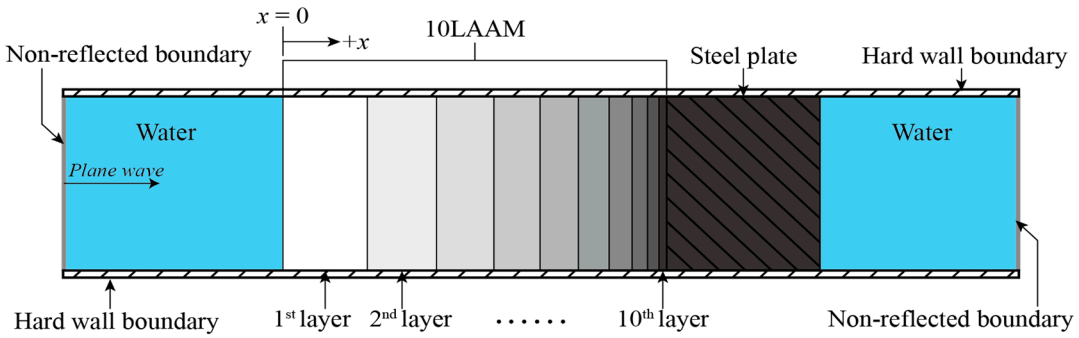


Figure 8. Numerical model for acoustic performance analysis of 10LAAM via 4MM.

Table 1. Material properties and thicknesses of each layer.

Layer No.	Density [kg/m^3]	Sound Speed [m/s]	Thickness [mm]	Loss Factor
1	1100	1500	11	0.23
2	1300	1400	9	
3	1400	1800	7.5	
4	2000	1200	6	
5	2500	1500	5	
6	3200	1700	4	
7	3800	1900	3	
8	4600	2000	2	
9	5000	2500	1.5	
10	6500	5000	1	

Density, Young's modulus, Poisson's ratio, loss factor and thickness of the steel plate are set to 7850 kg/m^3, 200 GPa, 0.3, 0.001, and 20 mm, respectively. Both sides of the

structure including 10LAAM and steel plate are assumed to be contacted with water, which is fresh water without salinity, the density and sound speed of which are 1000 kg/m^3 and 1500 m/s, respectively.

In 4MM analysis, each termination of the waveguide is considered in relation to non-reflected boundaries. The upper and lower walls of the waveguide are assumed in relation to hard wall boundaries. The incident plane wave generated at the left termination boundary propagates in x-direction. The analyses are conducted from 100 Hz to 4 kHz in frequency step of 100 Hz, and the sizes of the finite elements are smaller than 0.00625 m, which is 1/60 of wavelength of the maximum analysis frequency 4 kHz.

First, ER and TL characteristics of 10LAAM itself are calculated via 4MM and TMM to cross-validate the applicability of the methods. Then, ER and TL performances of 10LAAM with the steel back plate, which are used in a practical application example for an underwater vehicle model, are calculated via TMM and compared to those of 10LAAM itself.

4.2. Analysis Results and Discussion

ER and TL performances of 10LAAM itself evaluated using 4MM and TMM are shown in Figure 9.

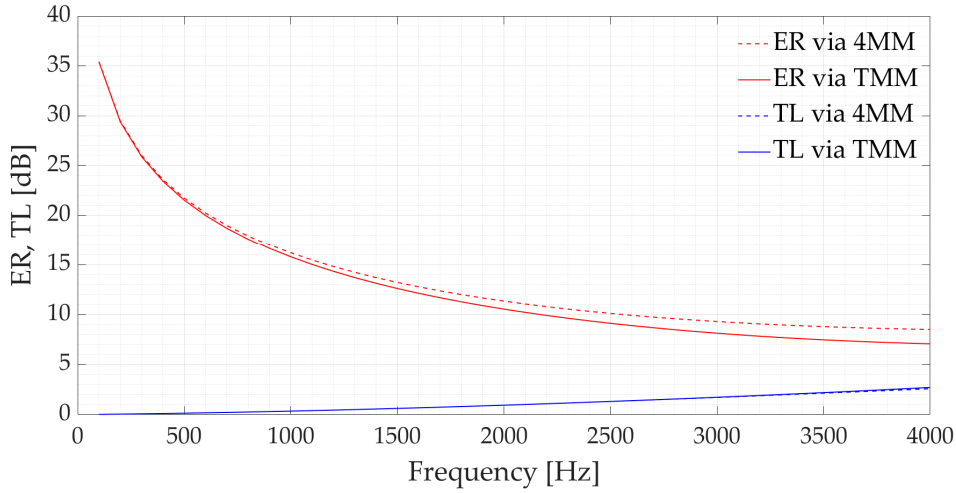


Figure 9. ER and TL performances of 10LAAM itself.

From the results, it is observed that discrepancies between both results become larger as frequency rises, and this is because TMM has some limitations in its application due to the relationship between the thickness of TSAM and incident wavelength. Nevertheless, ER and TL evaluation results via both methods show good agreements and similar tendencies to each other with maximum differences of 1.43 dB and 0.13 dB at 4 kHz on ER and TL, respectively. Meanwhile, computation times of the methods are represented in Table 2, and it is concluded that TMM is more suitable for the proposed simplified TS analysis procedure than 4MM because of the relatively low calculation and time costs required on the acoustic performance evaluation of TSAM.

Table 2. Computation times of 4MM and TMM on ER and TL analysis for 10LAAM itself.

	4MM	**TMM**
Computation time	3 min 53 s	0.8409 s

Additionally, ER and TL performances of the 10LAAM attached to the steel back plate are shown in Figure 10.

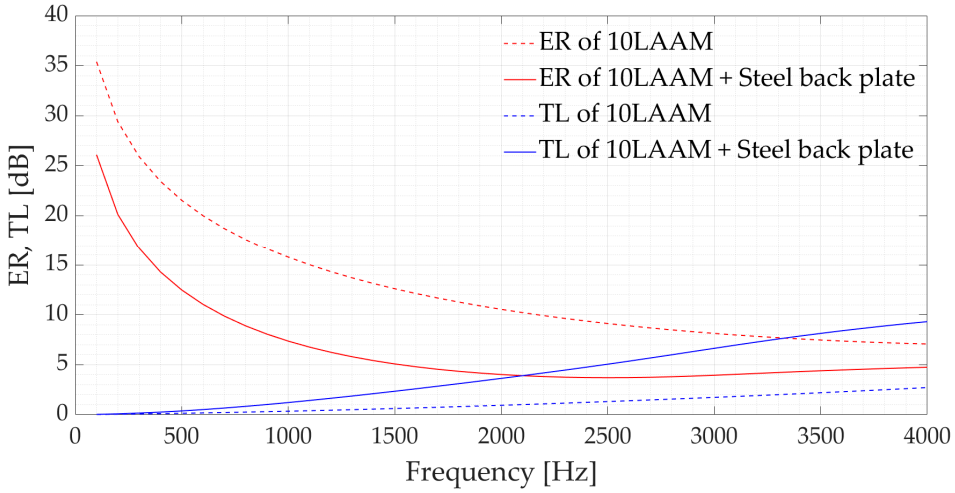


Figure 10. ER and TL of 10LAAM without and with the steel back plate evaluated by TMM.

From the results, the ER of 10LAAM with the back plate is evaluated lower than that without the plate because of the large acoustic impedance of steel compared to that of water. For the same reason, it is observed that the TL of 10LAAM with the back plate is increased compared to that without the plate.

In this study, ER and TL performances of 10LAAM with the steel back plate are used to investigate TS reduction effects for an underwater vehicle analysis model.

5. Application of the Proposed Procedure

To validate the applicability of the proposed simplified TS analysis procedure, practical application using the Benchmark Target Strength Simulation (BeTSSi) model is presented and TS reduction effects owing to 10LAAM are investigated through a series of TS analyses.

5.1. BeTSSi Model

The BeTSSi model simulates the geometric and acoustic characteristics of a 1700-ton former Soviet diesel submarine (Kilo class). This model is selected for its comprehensive representation of both the outer and inner structures of an underwater vehicle including its outer hull, pressure hull, sail, mast, functional sonar, bulkheads, torpedo tubes, and so forth. These features ensure the model sufficiently captures the geometric and acoustic complexities of realistic underwater vehicle designs. The BeTSSi model was proposed for verification of the performance of TS simulation software used by NATO countries and is widely utilized as a standard model for various TS analyses and reduction designs [1]. Future work could consider incorporating more complex geometric structures to reflect the design features of next-generation submarines. The outer structure whose length, breadth, and depth including the sail of the model are 62 m, 7 m, and 11 m, respectively, is shown in Figure 11 and the inner structure is shown in Figure 12.

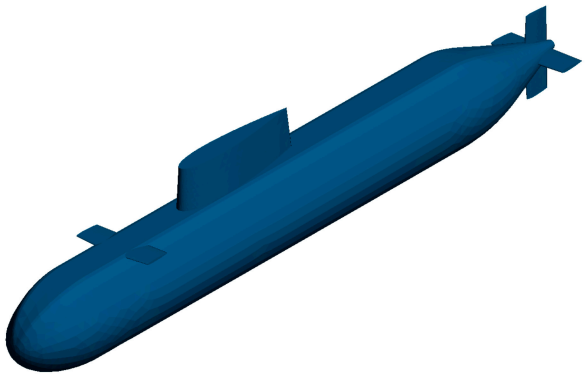


Figure 11. Outer structure of BeTSSi model.

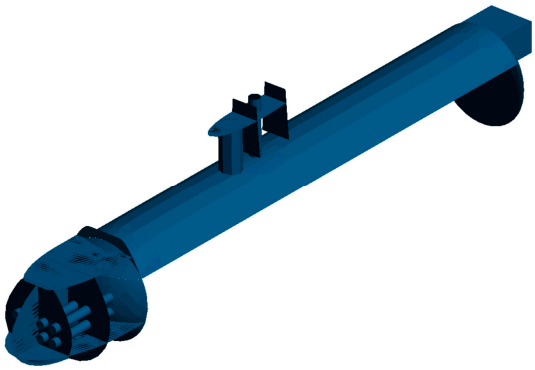


Figure 12. Inner structure of BeTSSi model.

5.2. TS Analysis Conditions

The TS of the BeTSSi model is analyzed based on PO/GO combined method with the analysis conditions represented in Table 3. Analysis range of azimuth angle is set to 0°–180° considering the geometrical symmetry of the model.

Table 3. TS analysis condition for the BeTSSi model.

Frequency	Range of Azimuth Angle	Max. Reflection Order	Elevation Angle
3 kHz	0° to 180° with 0.2° step	3	0°

The number of triangular elements consisting of the analysis models are represented in Table 4. Sizes of the elements are determined to accurately describe curvatures of the model surfaces by satisfying the condition that the distance between target surface and the corresponding element is below 1/16 of analysis wavelength. To ensure numerical convergence and stability of the TS analysis, this condition is validated by several simulations with varying distances between the target surface and element. From the simulation, it is shown that when the mesh resolution satisfies this condition; the TS analysis result exhibited changes below 0.5% between successive iterations. This confirms that the modeling approach and chosen element sizes not only describe the geometric complexities of the model but also ensure convergence of the numerical solution. The described approach guarantees both the accuracy of the curvature representation and the reliability of the analysis results.

Table 4. Number of the elements in the analysis model.

Numerical Analysis Model	Outer Structure	Inner Structure
Number of elements	26,054	27,283

To investigate TS reduction effects due to 10LAAM attached on the outer structure of the model, three cases of numerical studies are conducted. First, the TS of the BeTSSi model is analyzed with the assumption that both outer and inner structures are perfect reflectors, whose analysis case is named "Perfect reflector", and TS contributions according to reflection orders are studied. Second, the TS of the model whose outer structure consists of steel plates, namely "Steel plate" case, which have ER and TL characteristics shown in Figure 13 is analyzed.

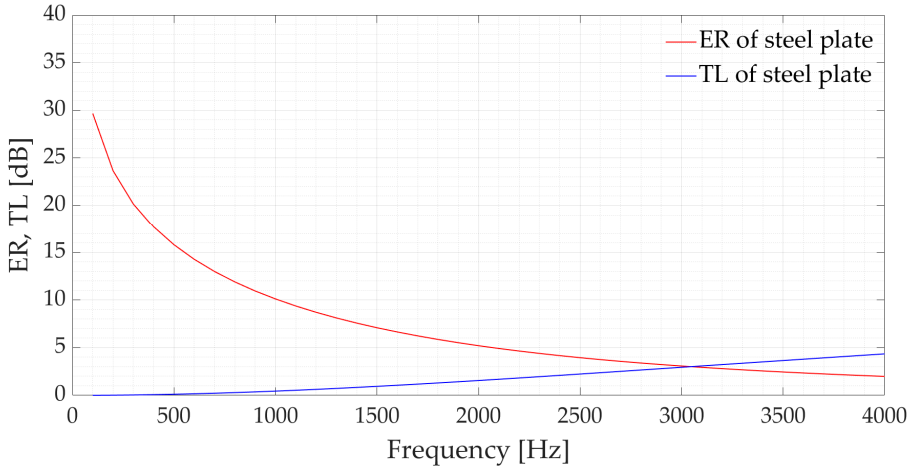
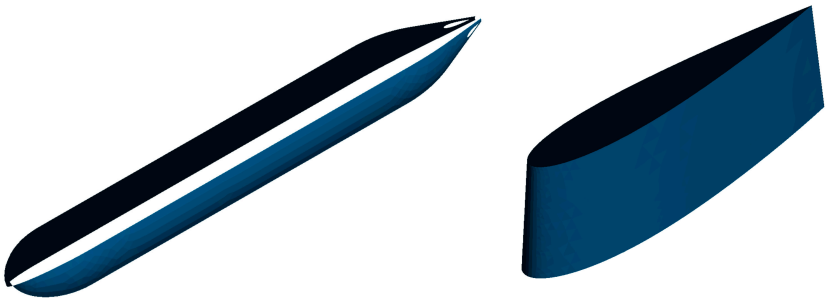


Figure 13. ER and TL characteristics of 20 mm steel plate.

Last, the TS of the model is analyzed when 10LAAM is attached on two parts of the outer structure shown in Figure 14, and the remaining consists of only steel plates, whose analysis case is named "Steel plate + 10LAAM". The attachment location of the 10LAAM shown in Figure 14a is determined considering that ER characteristics at the center of the outer hull, including vertical threat sector [2], significantly affect the TS of the entire model. In addition, 10LAAM is attached to the sail shown in Figure 14b since TL performance of the material can effectively reduce acoustic energies transmitted through the outer structure to the inner structure such as bulkheads, masts, and so forth.



(**a**) (**b**)

Figure 14. The 10LAAM attachment locations on outer structure of the BeTSSi model: (**a**) center of the outer hull (2292 triangular elements); (**b**) sail (1893 triangular elements).

Meanwhile, it is highly complicated to calculate multiple reflection effects of the inner structure when TS reduction methods are applied to only a part of the structure. Thus, most acoustic waves incident to the inner structure at elevation angle 0° are assumed to be transmitted through the outer structure that has 10LAAM on its surface; the TL characteristic of 10LAAM with a steel back plate shown in Figure 10 are uniformly considered in relation to the outer structure in TS analysis for the inner structure. Additionally, since it is difficult to

seek information on the material properties of the inner structure, the inner structure of the model is retained to be perfect a reflector in the second and the third analysis cases.

5.3. Analysis Results and Discussion

The TS analysis results for both outer and inner structures, which are considered as perfect reflectors, are shown in Figures 15 and 16, respectively, including TS contributions of the 1st, 2nd, and 3rd reflection components.

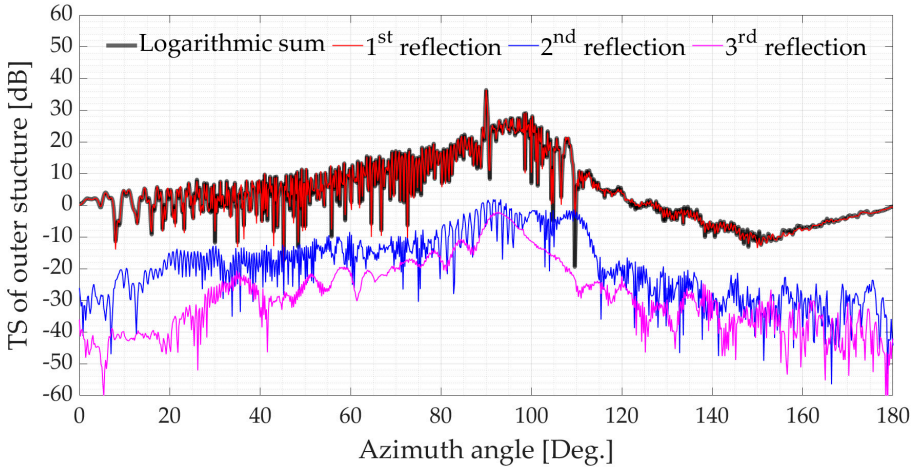


Figure 15. TS analysis results for perfect reflecting outer structure of the BeTSSi model.

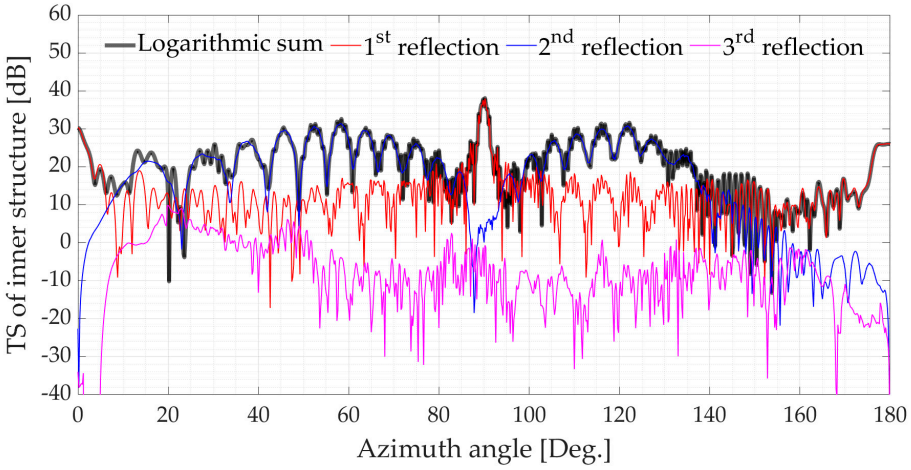


Figure 16. TS analysis results for perfect reflecting inner structure of the BeTSSi model.

From the results shown in Figure 15, it is confirmed that the first reflection component dominantly contributes to the TS of the outer structure at all azimuth angles against the other components. On the other hand, for the inner structure, it is observed that the first reflection component is dominant near incidence azimuth angles 0°, 90°, and 180°, which are facing the bow, midship, and stern sections, respectively, as shown in Figure 16. At the other azimuth angles, the second reflection component is relatively dominant because of the multi-reflection effects due to transverse bulkheads and torpedo tubes.

Figures 17 and 18 show the TSs of the outer and inner structures of the BeTSSi model, respectively, for three analysis cases. Figure 19 shows the total TS evaluation results of each analysis case, where they were calculated by logarithmic sums of TS contributions of the outer and inner structures.

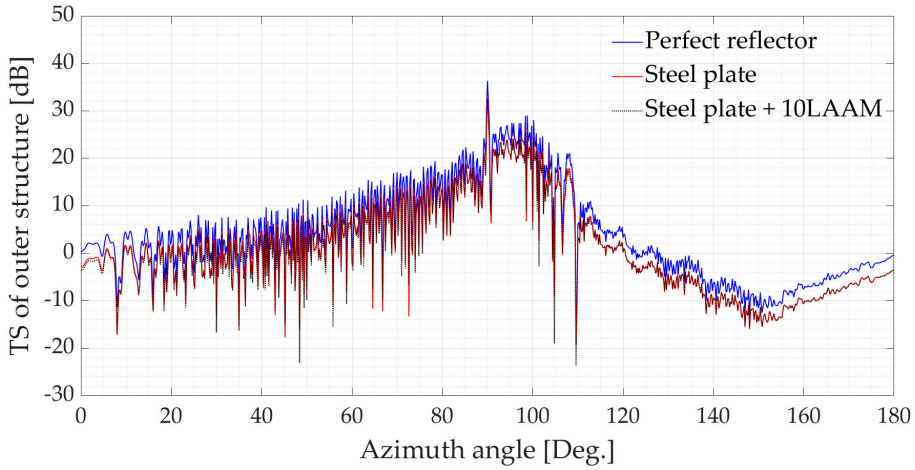


Figure 17. TS analysis results of the outer structure for three analysis cases.

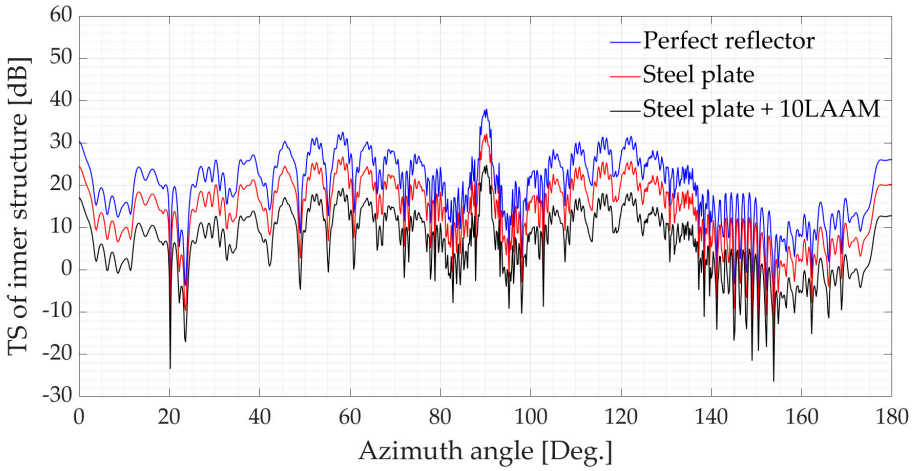


Figure 18. TS analysis results of the inner structure for three analysis cases.

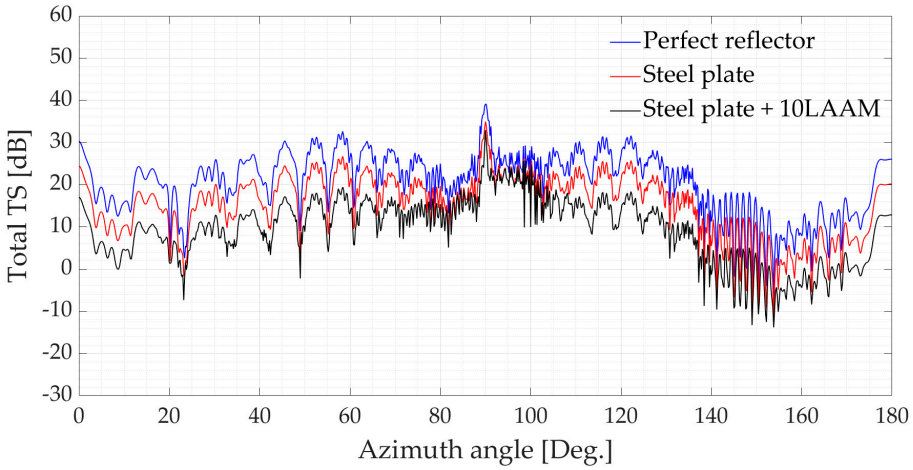


Figure 19. Total TS analysis results for three analysis cases.

From the results shown in Figure 17, it is observed that the overall TS evaluation results of the outer structure for the cases of "Steel plate" and "Steel plate + 10LAAM" are 3.1 dB and 3.4 dB lower than that for "Perfect reflector". It seems that partially attached 10LAAM contributed to the outer structure having slightly higher ER performance in the "Steel plate + 10LAAM" case compared to "Steel plate" case, since the ERs of steel plate itself and 10LAAM with steel back plate are 3.1 dB and 4.0 dB at 3 kHz, as shown in

Figures 10 and 13, respectively. In addition, from the results shown in Figure 18, the TSs of the inner structure for the "Steel plate" and "Steel plate + 10LAAM" cases were 5.9 dB and 13.3 dB lower than those of the "Perfect reflector" case. It is confirmed that the TL characteristics of them are doubled compared to the TLs of steel plate itself and 10LAAM with steel back plate, which are given as 2.9 dB and 6.6 dB at 3 kHz in Figures 10 and 13, respectively. This is because the acoustic waves incident to the inner structure is considered to transmit to the outer structure twice.

Meanwhile, it is observed that total TS of the "Steel plate + 10LAAM" case is globally lower than that of the "Steel plate" case, except near the azimuth angle of 90°, where the TS contribution of the outer structure was relatively dominant compared to that of the inner structure. This is because TS reduction effects owing to the attached acoustic material are largely caused by TL performance rather than the ER characteristics of 10LAAM with steel back plate.

Hence, it is deduced that the proposed simplified TS analysis procedure can be reliably applicable to not only TS analysis for underwater vehicles but also the investigation of TS reduction effects owing to TSAMs attached on the structures.

6. Conclusions

This study aims to suggest a simplified TS analysis procedure of an underwater vehicle considering TSAMs. The proposed procedure applies the ER and TL, which are the indicators representing the acoustic performance of TSAMs in the TS analysis. For the TS analysis, the outer structure and inner structure of the underwater vehicle are analyzed separately, with ER and twice the TL considered, respectively. The total TS of the underwater vehicle is calculated by logarithmic sums of TS contributions of the outer and inner structures determined above. To calculate the acoustic performance of TSAM, the ER and TL of 10-layer acoustic absorbing material are calculated and cross-validated via the transfer matrix method and 4-microphone method. The results of both methods show good agreements and similar tendencies to each other, but the transfer matrix method offers lower calculation and time costs than the 4-microphone method. Therefore, it is concluded that the transfer matrix method is more suitable for the proposed simplified TS analysis procedure than the 4-microphone method. To validate the applicability of the proposed procedure, the practical application using the BeTSSi model, which is standard model for various TS analyses, is presented. From the results regarding each structure of BeTSSi, which is considered as perfect reflector including TS contributions of the first, second, and third reflection components, it is confirmed that the first reflection is dominant for the outer structure at all azimuth angles. Meanwhile, for the inner structure, it is confirmed that the first reflection is dominant at certain azimuth angles and the second reflection is dominant at the others. Then, three cases of TS analyses are conducted according to the surface conditions of the outer structure of BeTSSi models. From the results, it can be confirmed that the performance of the TSAM is reflected in regard to the TS analysis and the TS of the BeTSSi model is reduced. For the results pertaining to the outer structure of the model, it is observed that overall TS evaluation results for the cases where the outer structure consists of a steel plate and the case where a steel plate with TSAMs are 3.1 dB and 3.4 dB lower; for the inner structure, these values are 5.9 dB and 13.3 dB lower compared to the case where the outer structure consists of a perfect reflector. Given the overall results of the validation and simulation, it is concluded that proposed procedure in this study could be reliably applicable to the TS analysis of underwater vehicles considering the acoustic performance of TSAMs.

Author Contributions: Conceptualization, J.K. (Jaeman Kim), J.K. (Jangwoo Kim), D.-S.C. and K.K.; methodology, J.K. (Jaeman Kim), J.K. (Jangwoo Kim), K.S., Y.-h.S. and K.K.; validation, J.K. (Jaeman

Kim), J.K. (Jangwoo Kim), J.-Y.L., K.S. and S.-J.P.; investigation, J.K. (Jangwoo Kim), J.K. (Jaeman Kim) and D.-S.C.; data curation, J.K. (Jangwoo Kim), J.K. (Jaeman Kim) and J.-Y.L.; writing—original draft, J.K. (Jangwoo Kim) and J.K. (Jaeman Kim); writing—review and editing, J.K. (Jangwoo Kim), J.K. (Jaeman Kim), J.-Y.L. and Y.-h.S.; supervision, K.S., Y.-h.S. and K.K. All authors have read and agreed to the published version of the manuscript.

Funding: Korea Research Institute for defense Technology planning and advancement (No. KRIT-CT-23-018).

Institutional Review Board Statement: Not applicable.

Data Availability Statement: The original contributions presented in the study are included in the article, further inquiries can be directed to the corresponding authors.

Acknowledgments: This work was supported by Korea Research Institute for defense Technology planning and advancement (KRIT) grant funded by the Korea government (DAPA (Defense Acquisition Program Administration)) (No. KRIT-CT-23-018, Laboratory of Advanced Maneuverability and Stealth Submarine, 2024).

Conflicts of Interest: The authors declare no conflict of interest.

References

1. Le Bras, Y. Target Echo Strength: Design options to reduce it. In Proceedings of the Undersea Defence Technology 2018 (UDT 2018), Glasgow, UK, 26–28 June 2018.
2. Avsic, T. A target echo strength reduction technique. In Proceedings of the 4th Underwater Acoustics Conference and Exhibition, Skiathos, Greece, 3–8 September 2017; pp. 419–430.
3. Ivansson, S.M. Sound absorption by viscoelastic coatings with periodically distributed cavities. *J. Acoust. Soc. Am.* **2006**, *119*, 3558–3567. [CrossRef]
4. Ivansson, S.M. Numerical design of Alberich anechoic coatings with superellipsoidal cavities of mixed sizes. *J. Acoust. Soc. Am.* **2008**, *124*, 1974–1984. [CrossRef] [PubMed]
5. Zhao, D.; Zhao, H.; Yang, H.; Wen, J. Optimization and mechanism of acoustic absorption of Alberich coatings on a steel plate in water. *Appl. Acoust.* **2018**, *140*, 183–187. [CrossRef]
6. Liu, R.; Pei, D.; Wang, Y. Experimental research on sound absorption properties of impedance gradient composite with multiphase. In Proceedings of the International Conference on Novel Functional Materials, Shanghai, China, 8–9 November 2029; p. 012009.
7. Lee, D.; Jang, Y.; Park, J.; Kang, I.S.; Li, J.; Rho, J. Underwater stealth metasurfaces composed of split-orifice–conduit hybrid resonators. *J. Appl. Phys.* **2021**, *129*, 105103. [CrossRef]
8. Shi, K.; Jin, G.; Liu, R.; Ye, T.; Xue, Y. Underwater sound absorption performance of acoustic metamaterials with multilayered locally resonant scatterers. *Results Phys.* **2019**, *12*, 132–142. [CrossRef]
9. Zhang, Y.; Cheng, L. Ultra-thin and broadband low-frequency underwater acoustic meta-absorber. *Int. J. Mech. Sci.* **2021**, *210*, 106732. [CrossRef]
10. Gao, N.; Lu, K. An underwater metamaterial for broadband acoustic absorption at low frequency. *Appl. Acoust.* **2020**, *169*, 107500. [CrossRef]
11. Jiang, H.; Wang, Y. Phononic glass: A robust acoustic-absorption material. *J. Acoust. Soc. Am.* **2012**, *132*, 694–699. [CrossRef] [PubMed]
12. Qu, S.; Gao, N.; Tinel, A.; Morvan, B.; Romero-García, V.; Groby, J.-P.; Sheng, P. Underwater metamaterial absorber with impedance-matched composite. *Sci. Adv.* **2022**, *8*, eabm4206. [CrossRef]
13. Humphrey, V.F.; Robinson, S.P.; Smith, J.D.; Martin, M.J.; Beamiss, G.A.; Hayman, G.; Carroll, N.L. Acoustic characterization of panel materials under simulated ocean conditions using a parametric array source. *J. Acoust. Soc. Am.* **2008**, *124*, 803–814. [CrossRef] [PubMed]
14. *ISO 10534-1*; Acoustics-Determination of Sound Absorption Coefficient and Impedance in Impedance Tubes, Part 1: Method Using Standing Wave Ratio. ISO (International Organization for Standardization): Geneva, Switzerland, 1996.
15. Niresh, J.; Neelakrishnan, S.; Subharani, S.; Kannaian, T.; Prabhakaran, R. Review of acoustic characteristics of materials using impedance tube. *ARPN J. Eng. Appl. Sci* **2015**, *10*, 3319–3326.
16. Kunio, J.; Yoo, T.; Jou, K.; Bolton, J.; Enok, J. A comparison of two and four microphone standing wave tube procedures for estimating the normal incidence absorption coefficient. In Proceedings of the 38th International Congress and Exposition on Noise Control Engineering, Ottawa, ON, Canada, 23–26 August 2009; pp. 1057–1065.

17. Barnard, A.R.; Rao, M.D. Measurement of sound transmission loss using a modified four microphone impedance tube. In Proceedings of the ASME Noise Control and Acoustics Division (Noise-Con'04), Baltimore, MD, USA, 12–14 July 2004; pp. 206–216.
18. Lee, S.-S.; Jang, J.-Y.; Song, K. Enhanced acoustic attenuation in a coiled meta-silencer: Broadband low-frequency noise control through rainbow trapping. *Mech. Syst. Signal Process.* **2025**, *222*, 111744. [CrossRef]
19. Dell, A.; Krynkin, A.; Horoshenkov, K. The use of the transfer matrix method to predict the effective fluid properties of acoustical systems. *Appl. Acoust.* **2021**, *182*, 108259. [CrossRef]
20. Ye, C.; Liu, X.; Xin, F.; Lu, T.J. Influence of hole shape on sound absorption of underwater anechoic layers. *J. Sound Vibr.* **2018**, *426*, 54–74. [CrossRef]
21. Urick, R.J. *Principles of Underwater Sound*, 3rd ed.; Peninsula Publishing: Westport, CT, USA, 1983.
22. Okumura, T.; Masuya, T.; Takao, Y.; Sawada, K. Acoustic scattering by an arbitrarily shaped body: An application of the boundary-element method. *ICES J. Mar. Sci.* **2003**, *60*, 563–570. [CrossRef]
23. Thompson, L.L.; Pinsky, P.M. A space-time finite element method for the exterior acoustics problem. *J. Acoust. Soc. Am.* **1996**, *99*, 3297–3311. [CrossRef]
24. Kim, K.-H.; Kim, J.-H.; Cho, D.-S. RCS analysis of complex structures using object precision method. *J. Soc. Nav. Archit. Korea* **2005**, *42*, 159–164.
25. Kim, K.-H.; Cho, D.-S.; Kim, J.-C. High frequency acoustic scattering analysis of underwater target. *J. Soc. Nav. Archit. Korea* **2005**, *42*, 528–533.
26. Klement, D.; Preissner, J.; Stein, V. Special problems in applying the physical optics method for backscatter computations of complicated objects. *IEEE Trans. Antennas Propag.* **1988**, *36*, 228–237. [CrossRef]
27. Knott, E.F.; Schaeffer, J.F.; Tulley, M.T. *Radar Cross Section*, 2nd ed.; SciTech Publishing: Hampshire, UK, 2004.
28. Griesser, T.; Balanis, C. Backscatter analysis of dihedral corner reflectors using physical optics and the physical theory of diffraction. *IEEE Trans. Antennas Propag.* **1987**, *35*, 1137–1147. [CrossRef]
29. Kim, K.-H.; Cho, D.-S.; Seong, W.-J. Simulation of time-domain acoustic wave signals backscattered from underwater targets. *J. Acoust. Soc. Korea* **2008**, *27*, 140–148.
30. Kwon, H.-W.; Hong, S.-Y.; Kim, H.-M.; Song, J.-H. Analysis of acoustic target strength for the submarine with Alberich anechoic coating effects. *J. Korean Soc. Mar. Environ. Saf.* **2013**, *19*, 410–415. [CrossRef]

Disclaimer/Publisher's Note: The statements, opinions and data contained in all publications are solely those of the individual author(s) and contributor(s) and not of MDPI and/or the editor(s). MDPI and/or the editor(s) disclaim responsibility for any injury to people or property resulting from any ideas, methods, instructions or products referred to in the content.